JOURNAL OF OPTOELECTRONICS AND ADVANCED MATERIALS Vol. 9, No. 11, November 2007, p. 3645 - 3650

Molecular sieves SBA-15 type doped with heteropolyacids: textural and structural properties

A. POPA[*,a], V. SASCA[a], E. E. KIŠ[b], RADMILA MARINKOVIĆ-NEDUČIN[b], J. HALASZ[c]
[a]*Institute of Chemistry Timişoara, Bl.Mihai Viteazul 24, 300223 Timisoara, Romania*
[b]*University of Novi Sad, Faculty of Technology, Cara Lazara 1, Novi Sad, Serbia*
[c]*University of Szeged, Dep.of Applied and Environmental Chemistry, Rerrich ter 1, H-6720 Szeged, Hungary*

In order to be more effective for catalytic reactions, heteropolyacids (HPAs) are usually impregnated on different porous materials with high surface area. Highly dispersed heteropolyacids species, $H_3PMo_{12}O_{40}$ and $H_4PVMo_{11}O_{40}$ were supported on SBA-15 and Ti- SBA 15 molecular sieves. All supported HPAs were prepared by impregnation using the incipient wetness techniques with a mixture water: ethanol = 1:1. The structure and texture of $H_3PMo_{12}O_{40}$ and $H_4PVMo_{11}O_{40}$ supported on SBA 15 and Ti- SBA 15 were studied by XRD, FT-IR, low temperature nitrogen adsorption and scanning electron microscopy SEM with EDS. FT-IR studies showed that HPAs anions preserved their Keggin structure after deposition on SBA-15 and Ti- SBA 15 supports. X-ray diffraction and SEM studies confirmed the uniformity of the distribution of active phase in the catalyst samples. The values of specific surface area of both HPAs were increased by deposition on molecular sieve supports. It is found that most of HPMo and HPVMo (active phases) in samples are well dispersed on the support and SBA-15 supported HPA still keeps its Keggin structure. The surface morphology of the SBA-15 supported samples is almost similar to that of SBA-15 support. A relatively uniform distribution of active phase in the support pores was evidenced by EDS analysis.

(Received May 9, 2007; accepted November 1, 2007)

Keywords: Heteropolyacids, Molecular sieves, Texture, Structure, BET, SEM, XRD

1. Introduction

In recent years, heteropolyacids (HPAs) with Keggin structure have been applied to catalyse a large spectrum of chemical reactions ranging from selective oxidation processes to acid-catalyzed transformation of organic molecules, both in the heterogeneous and homogeneous systems [1-4]. Pure HPAs generally show low catalytic reactivity owing to their small surface area. In order to be more effective for catalytic reactions, HPAs are usually impregnated on different porous materials with high surface area (silica, titania, polymers, molecular sieves) [5-11].

SBA-15 is a relatively new discovered mesoporous molecular sieve with uniform tubular channels whose pore diameter can be engineered in the range from 50 to 300 Å, which allow the easy introduction of HPAs molecules (12 Å diameter). Compared with MCM-41 molecular sieve, SBA-15 has larger pore diameter, thicker pore wall and higher hydrothermal stability [12-13].

In the literature very few references have been reported concerning $H_3[PMo_{12}O_{40}]$ and $H_4[PMo_{11}VO_{40}]$ supported on SBA 15 mesoporous silicate, majority of the studies been focused on investigation the most acidic HPAs in the series, namely $H_3PW_{12}O_{40}$ (HPW) [14-20].

Yang and al. [14] were used two types of preparation: directly synthesized HPW-SBA15 composites by sol-gel method and SBA-15 supported HPW. According to XRD patterns no characteristic peaks of HPW are observed for HPW-SBA15 composites, indicating that HPW is finely dispersed on the surface of the sample or incorporated in the pore walls of the sample. The introduction of HPW decreases the surface area, total pore volume and pore size of pure SBA-15. Such decrease is sharp for SBA-15 supported HPW due to large quantity of active phase existing in the channels, on the surface or on the pore walls.

Two types of preparation procedures were used to study HPW-SBA-15 composites: by impregnation of mesoporous material SBA-15 with different amounts of HPW, and by directly synthesizing HPW-containing SBA-15 in non-aqueous (ethanol) medium at room temperature [15]. The impregnated high dispersed HPW favoured the selectivity of acetic anhydride catalytically condensed from acetic acid and the bigger the pore size, the better selectivity. For the directly synthesized HPW-containing SBA-15 the selectivity was increased to 96% over the composites with 6.4 wt.% of chemically bound HPW.

HPW could highly be dispersed on the surface of the mesopore walls of SBA-15 until the HPW loading is as high as 60 wt.% with the mesoporous structure of SBA-15 being preserved [16]. The effect of grafting the alumina species at the surface of silica on HPW immobilization capacity and performance of HPW composites in acid-catalysed reactions were studied with regular silica-gel and mesostructured silica SBA-15 [17, 18]. Grafting of silica with small alumina clusters at partial coverage produces isolated basic sites with the same strength as at the pure alumina surface. It affords a monodentate adsorption of molecular HPW and causes a strong enough immobilization of HPW at the solid surface to prevent its leaching in polar reactant solutions. Using mesostructured SBA-15 as support yields optimized catalysts with 30-70% higher activity compared with that based on regular silica

gel. This is a result of higher surface area and surface concentration of silanols in SBA-15.

The characteristics as sorbents for HPW-SBA15 and HPMo-SBA15 composites were tested comparatively with HPW- mesoporous synthetic carbon (Sibunit) for ammonia and amines adsorption [20]. HPW-SBA15 and HPMo-SBA15 composites have relatively narrow pore size distribution and open porous structure, whereas mesoporous carbon Sibunit has bottle-neck type pores. HPW-SBA15 and HPMo-SBA15 composites have higher total ammonia uptake than Sibunit material, therefore these composites being promise materials for removal of ammonia and amines from air streams at very low concentrations.

In the selective oxidation of unsaturated aldehydes and of low alcohols most frequently used are molybdophosphoric acid $H_3[PMo_{12}O_{40}]\cdot xH_2O$ (HPMo) and 1-vanado-11-molybdophosphoric acid $H_4[PMo_{11}VO_{40}]\cdot yH_2O$ (HPVMo) in consequence of their high catalytic activity. In order to obtain highly dispersed heteropolyacids species, HPMo and HPVMo were supported on SBA 15 and Ti- SBA 15. The goal of this work was to characterise the texture and structure of these heteropolyacids supported on SBA 15 and Ti- SBA 15 in reference to the bulk solid heteropolyacids.

2. Experimental

$H_4[PMo_{11}VO_{40}]\cdot 12H_2O$ was prepared by two methods: Tsigdinos and hydrothermal method [2-3]. In both cases, HPVMo was crystallized slowly from aqueous solutions at room temperature. $H_3[PMo_{12}O_{40}]\cdot 13H_2O$ was purchased from Merck. The as-received material was recrystallized prior to use. They are stable at room temperature with 12-14 H_2O molecules. Mesoporous silica SBA-15 was synthesized according to the procedure developed by D.Zhao and colab. [12].

The HPAs active phase deposition on SBA 15 and Ti-SBA 15 (Si/Ti = 50) molecular sieves was performed by impregnation from water: ethanol = 1:1 solution. The HPMo and HPVMo acids were deposited in the concentration of 15 and 30 wt. % loading.

The structure and texture of HPMo and HPVMo supported on molecular sieve was studied by XRD, FT-IR, low temperature nitrogen adsorption and scanning electron microscopy with EDS analysis.

Textural characteristics of the outgassed samples were obtained from nitrogen physisorption using a Quantachrome instrument, Nova 2000 series. The specific surface area S_{BET}, mean cylindrical pore diameters d_p and adsorption pore volume V_{pN2} were determined. Prior to the measurements the samples were degassed to 10^{-5}Pa at 250ºC. The BET specific surface area was calculated by using the standard Brunauer, Emmett and Teller method on the basis of the adsorption data. The pore size distributions were calculated applying the Barrett-Joyner-Halenda (BJH) method to the desorption branches of the isotherms. The IUPAC classification of pores and isotherms were used in this study.

Microstructure characterisation of the catalyst particles was carried out with a JEOL JSM 6460 LV instrument equipped with an Oxford Instruments EDS analyser. Powder materials were deposited on adhesive tape fixed to specimen tabs and then ion sputter coated with gold.

Powder X-ray diffraction patterns were recorded between $2\theta = 0.5\div5°$ and $2\theta = 5\div60°$, respectively, on a XD 8 Advanced Bruker diffractometer using Ni-filtred Cu K_α radiation source at 40 kV and 20 mA with a scan rate of 0.02º.

The IR absorption spectra were recorded with a Jasco 430 spectrometer (spectral range 4000-400 cm^{-1} range, 256 scans, and resolution 2 cm^{-1}) using KBr pellets.

3. Results and discussion

The XRD patterns of SBA 15 and the two HPA/ SBA 15 samples are shown in Fig. 1 and the data are presented in Table 1. The patterns show the characteristics of a typical mesoporous SBA 15 structure. The hexagonal structure of SBA 15 is confirmed by the presence of three diffraction peaks at low angles of 0.9º, 1.56º and 1.76º, corresponding to the Miller crystal planes (100), (110) and (200), respectively [12].

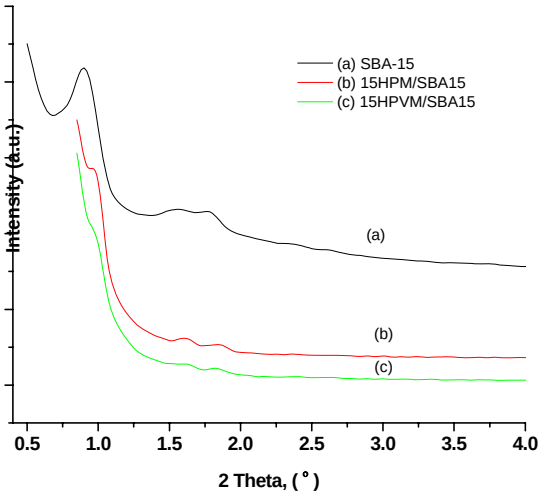

Fig. 1. X-ray diffraction pattern of SBA 15 molecular sieves and supported HPAs: a) SBA 15, b) 15HPMo/ SBA 15, c) 15HPVMo/ SBA 15.

The d_{100} diffraction peak of SBA 15 supported HPMo and HPVMo are shifted towards lower values compared to its SBA 15 analogue. As in the case of HPW/ SBA 15 [15-18] the amount of HPMo or HPVMo has an important effect on the intensity of the main reflection peacks of the SBA 15 support, and the peaks height is inversely proportional to the amount of loaded HPAs. The XRD diffraction patterns of supported HPAs do not show any bulk HPAs crystal phases, indicating that active phase is finely dispersed on the SBA 15 support.

For Ti-SBA15 all three diffraction peaks at low angles are presented but with diminished intensity. The d_{100} diffraction peak of Ti-SBA15 and Ti-SBA15 supported HPAs appear like a shoulder. It can be asserted that the long – range order of Ti-SBA 15 is decreased evidently for loading of 30 wt. % HPAs.

The nitrogen adsorption isotherms of heteropolyacids supported on SBA 15 are shown in Fig. 2a. For SBA 15 molecular sieves and HPAs supported on SBA 15 one observe a type IV isotherm with a type H1 hysteresis loop in the high range of relative pressure. For the values of relative pressure in the range 0.6-0.8, the condensation process take place giving a sharp adsorption volume increase. This behavior indicates that this sample has a mesoporous character. The position of the inflection point of adsorption branch is related to the diameter of the mesopore, while the sharpness of the hysteresis loop shows the uniformity of the mesopore size distribution. Both HPMo and HPVMo heteropolyacids supported on SBA 15 present the type IV isotherm with a type H1 hysteresis loop.

Table 1. Textural properties of molecular sieves and supported HPAs.

Sample	XRD d_{100} d-spacing (Å)	Unit cell, a_o (Å)	Surface area (m^2/g)	Average pore diameter BJH_{Des} (Å)	Pore volume BJH_{Des} (cc/g)
SBA-15	98.1	113.3	725.6	60.1	1.19
15% HPMo/ SBA-15	92.0	106.2	534.3	59.7	0.92
15% HPVMo/ SBA-15	90.1	104.0	550.9	60.1	0.91
Ti-SBA-15	94.9	109.6	615.1	53.0	1.19
30% HPMo/ Ti-SBA-15	90.1	104.1	267.8	35.9	0.39
30% HPVMo/ Ti-SBA-15	91.9	106.1	345.3	34.4	0.42

The pore size distributions were calculated by Barret-Joyner-Halenda (BJH) method applied to the desorption branches of the isotherms. The pore size distribution curves of SBA 15 support and HPMo and HPVMo supported on SBA 15 have narrow pore size distribution within mesopore range with a maximum at approximatively 60 Å (Fig. 2b). The average pore size does not significantly change with HPAs impregnation only slightly variation of the values around the SBA-15 sample being observed (Table 1 and Fig. 2b).

After HPAs impregnation the pore volumes of samples decreased with the increase of the concentration of active phase and also the surface area decreased with the increase in HPAs loading.

In the case of HPAs supported on Ti-SBA-15 the irregular form of hysteresis loop in the relative pressure range 0.45-0.55 indicates the presence of nonuniformity in pores size and/or shape (Fig. 3a). The pore size distribution curves of HPMo and HPVMo supported on Ti-SBA 15 have two maximums within mesopore range at approximatively 35 and 52 Å showing the enlargement of the pore size (Fig. 3b).

In order to confirm the presence of the Keggin anion on SBA 15, the supported HPAs samples were analysed by FTIR. The $PMo_{12}O_{40}^{3-}$ Keggin ion structure consists of a PO_4 tetrahedron surround by four Mo_3O_{13} formed by edge-sharing octahedra. These groups are connected each other by corner-sharing oxygen. This structure give rise to four types of oxygen, being responsible for the fingerprints bands of Keggin ion between 1200 and 700 cm^{-1}.

The pure HPAs show an IR spectrum with the specific bands of the Keggin structure containing the main absorption lines at 1064 cm^{-1}, 961 cm^{-1}, 868 cm^{-1}, 783 cm^{-1} assigned to the stretching vibrations ν_{as} P -O, ν_{as} Mo=O_t, ν_{as} Mo-O_c-Mo and ν_{as} Mo-Oe-Mo [9, 11]. These bands are preserved on the supported samples, but they are broadened and partially obscured because of the strong absorption bands of SBA-15 (1082, 959, 802 and 463cm^{-1}) (Fig. 4).

The introduction of Ti cation into the SBA support slightly influenced the structure of molecular sieve. The vibration band at ca. 1082 cm^{-1} can be assigned to ν_{as}(Si-O-Si) and increased to 1089 cm^{-1} by incorporation of the metal into the structure of the Ti-SBA-15. The band at ca. 959 cm^{-1} present in the spectrum of SBA-15 sample can be assigned to the Si-O stretching vibration of $Si\text{-}O^-R^+$ group ($R^+ = H^+$), while in the Ti-SBA-15 spectra the band is shifted to 955 cm^{-1} and could be assigned to a ν_{as}(Si-O-Me) vibration. The bands at 802 and 463 cm^{-1} can be assigned to ν_s (Si-O-Si) and δ(Si-O-Si) bonds, respectively [21].

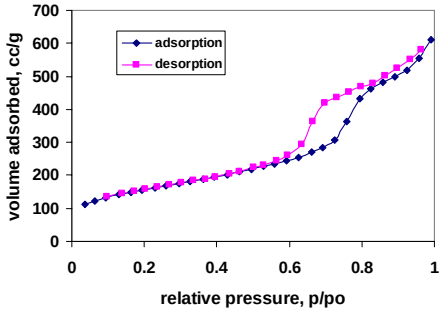

a

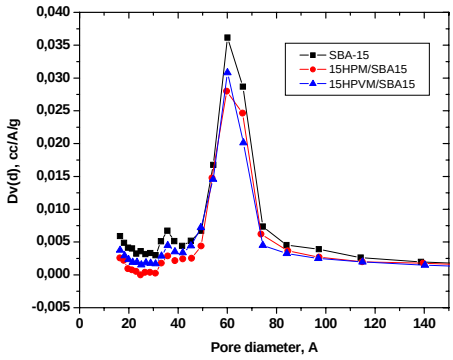

b

Fig. 2. Nitrogen adsorption-desorption isotherms of 15HPVMo/ SBA 15 at 77 K (a) and pore size distribution of HPAs supported on SBA 15 (b).

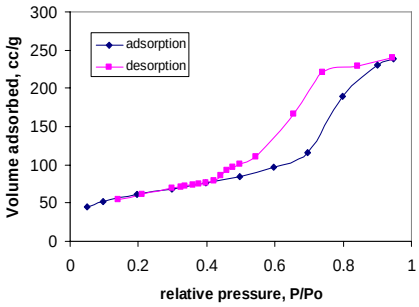

a

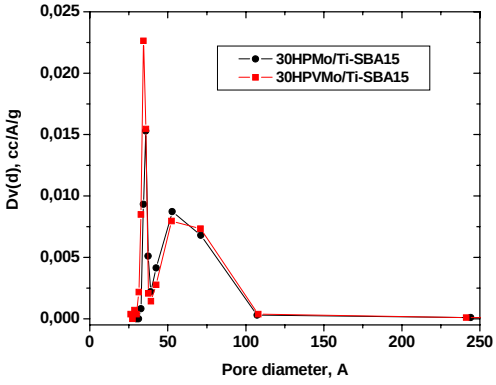

b

Fig. 3. Nitrogen adsorption-desorption isotherms of 30 HPMo / Ti-SBA 15 at 77 K (a) and pore size distribution of HPAs supported on Ti-SBA 15 (b).

Some of the bands of supported HPAs in the 1300-400 cm^{-1} region are partially or completely overlapped by the bands of the SBA-15 support (Fig. 4). The band assigned to the P –O asymmetric stretching vibration at 1064 cm^{-1} is completely overlapped by the strong band at 1082 cm^{-1} of the SBA-15. Two strong bands in the spectra of supported HPMo and HPVMo appeared at 960 and 809 cm^{-1}, as a result of the overlapping of the absorption bands of mesoporous silica at 959 and 802 cm^{-1} and those of HPAs at 961 and 783 cm^{-1}, respectively. A band with moderate intensity was observed at 881 cm^{-1} which corresponds to the ν_{as} Mo-O_c-Mo band vibration which appears at 868 cm^{-1} in the HPAs spectra. Therefore, the Keggin unit would be mainly characterized by the stretching vibrations assigned to terminal Mo=O_t and bridging Mo-O_c-Mo and Mo-Oe-Mo bonds.

The replacing of a Mo atom with a V one leads to the appearance of two "shoulders" corresponding to the absorption maxim of the vibration ν_{as} (P-O_p) at 1080 cm^{-1} and ν_{as} (V-O_t) at 980 cm^{-1}. This confirms the presence of V^{5+} inside the MO_6 octahedral. These shoulders could not be seen in the IR spectra of supported HPAs, because adsorption bands of mesoporous SBA-15 silica overlap them completely.

Finally, it could be assumed that Keggin structure of HPAs is preserved on the SBA-15 and on the Ti-SBA-15 supports, as evidenced by the agreement between the IR bands of parent and supported HPAs.

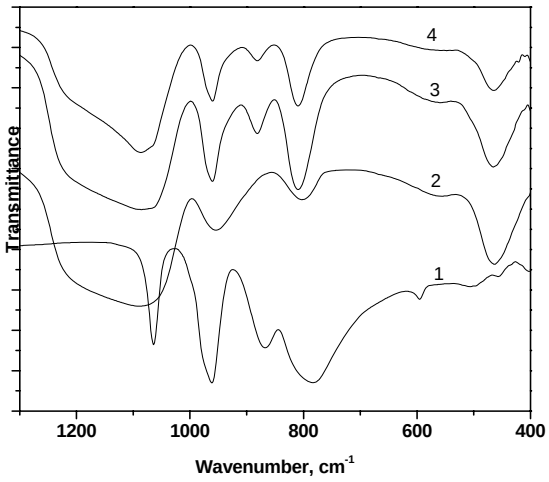

Fig. 4. FTIR spectra of 1) HPVMo, 2) Ti-SBA-15, 3) HPMo/Ti-SBA-15, 4) HPVMo/Ti-SBA-15.

SBA 15 and Ti- SBA 15 supports are composed of agglomerates of irregular shape particles with an average diameter below 0.5 μm (Fig. 5a). The surface morphology of SBA 15-supported HPAs is practically identical to that of the pure molecular sieves (Fig. 5b). From SEM images one can see that no separate crystallites of the bulk phase of HPAs were found in the supported samples.

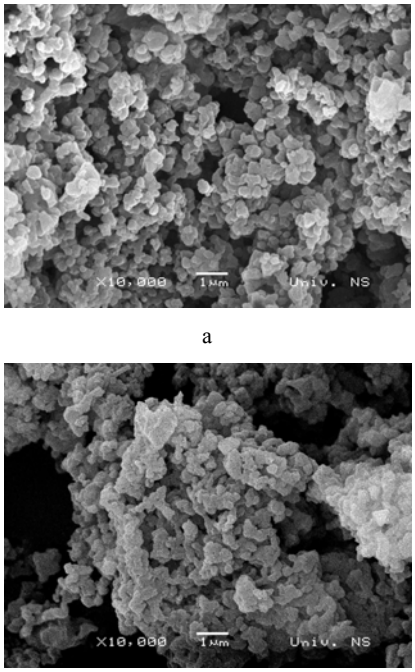

Fig. 5. SEM micrografs of Ti-SBA 15 (a) and HPMo/ Ti-SBA 15 (b).

HPAs distribution on supported samples surface was analysed by EDS method, which was performed as point analysis on thin particles. By this technique were obtained the chemical composition of silicon from SBA-15, silicon and titanium from Ti-SBA-15 and Mo, V and P elements of heteropolyacid. The EDS point analysis was made over several domains with 10×10 μm dimensions on the same sample. The analysis was repeated on different samples in order to ensure the reproducibility of the obtained results.

Microanalitycal data of EDS analysis show that the molybdenum and phosphorous (15 wt.% HPMo/ SBA-15) and molybdenum, phosphorous and vanadium (15 wt.% HPVM/ SBA-15) content is homogeneous and close to stoichiometric values.

In the case of SBA-15 supported HPMo the content of Mo as % wt. is 10.4 (stoichiometric value is 9.5), while P content is 0.31 (stoichiometric value is 0.25). For SBA-15 supported HPVMo the content of Mo as % wt. is 9.36 (stoichiometric value 8.9), P content is 0.28 (stoichiometric value is 0.26) and V content is 0.39 (stoichiometric value is 0.42) (Fig. 6 a, b).

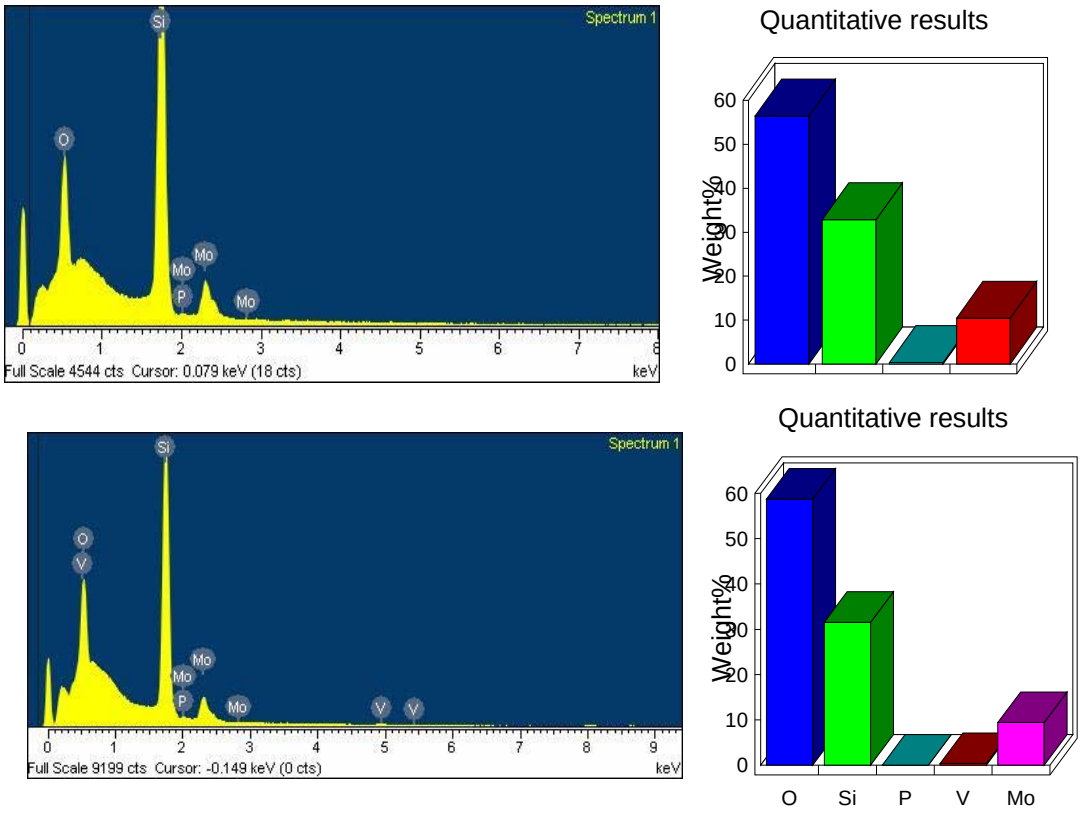

Fig. 6. a, b Microanalytical data of a 10×10 μm area and quantitative results of 15HPMo/SBA-15 (a) and HPVMo/ SBA-15 (b).

EDS analysis of Ti-SBA15 supported HPMo (30 wt. %) shows that the concentration of Mo is 17.11 wt. % (stoichiometric value is 18.9), while the P content is 0.37 wt. % (stoichiometric value is 0.50). It could be observed that 30HPMo/Ti-SBA15 exhibit a higher deviation of Mo and V concentration values from the stoichiometric ones, probably owing to higher active phase concentration supported at the surface of molecular sieve.

4. Conclusions

HPAs anions preserved their Keggin structure on the SBA15 and Ti-SBA15 surface and forms finely dispersed HPAs species. No HPAs detectable crystal phase is observed at 30 wt.% loading by XRD and SEM analysis. The SBA15 host material suffers structural distortions at higher loadings, which leads to a loss in long range order.

Both SBA15 supported HPAs exhibit differential pore size distribution in the mesoporosity range with a maximum at approximatively 60 Å. The surface area and pore size diameter of supported HPAs decreases with increase in HPAs loading due to the blockage of particles in mesopores of molecular sieve.

Keggin structure of HPAs is preserved on the SBA-15 and on the Ti-SBA-15 supports, as evidenced by the agreement between the IR bands of parent and supported HPAs.

The data of EDS analysis show that the molybdenum and phosphorous (15 wt.% HPMo/ SBA-15) and molybdenum, phosphorous and vanadium (15 wt.% HPVM/SBA-15) content is homogeneous and close to stoichiometric values.

References

[1] N. Mizuno, M. Misono, Chem. Rev. **98,** 199 (1998).
[2] M. Misono, Catal.Rev.-Sci.Eng. **29,** 269 (1987).
[3] F. Cavani, Catal. Today **41,** 73 (1998).
[4] E. Cadot, C. Marshal, M. Fournier, A. Teze, G. Herve, in Polyoxometalates, M. T.Pope, A. Muller (eds), Kluwer Acad. Publish., Dordrecht, p. 315 (1994).
[5] C. Marchal, A. Davidson, R. Thouvenot, G. Herve, J. Chem. Soc. Faraday Trans. **89,** 3301 (1993).
[6] S. Kastelan, E. Payen, J. B. Moffat, J. Catal. **125**, 45 (1990).
[7] A. Popa, V. Sasca, E. E. Kiss, Radmila Marinkovic-Neducin, M. T. Bokorov, J. Halasz, J. Optoelectron. Adv. Mater. **7**(6), 3169 (2005).
[8] A. Popa, V. Sasca, M. Stefănescu, E. E. Kis, R. Marinković-Nedučin, J. Serb. Chem. Soc. **71**(3), 235 (2006).
[9] A. Popa, V. Sasca, Radmila Marinković-Nedučin, Erne E. Kis, Rev. Roum.Chim. **51**(3), 211 (2006).
[10] A. Popa, Nicoleta Pleşu, V. Sasca, E. E. Kiš, Radmila Marinković-Nedučin, J. Optoelectron. Adv. Mater. **8**(5), 1944 (2006).
[11] A. Popa, V. Sasca, E. E. Kis, R. Marinković-Nedučin, M. T. Bokorov, J. Halasz, J. Optoelectron. Adv. Mater. **8**(3), 1317 (2006).
[12] D. Zhao, Q. Huo, J. Feng, B. F. Chmelka, G. D. Stucky, J. Am. Chem. Soc. **120**, 6024 (1998).
[13] Y. Chen, Y. Huang, J. Xiu, X. Han, X. Bao, Appl. Catal. A: General **273**, 185 (2004).
[14] L. Yang, Y. Qi, X. Yuan, J. Shen, J. Kim, J. Mol. Catal. A: Chemical **229**, 199 (2005).
[15] N. Y. He, C. S. Woo, H. G. Kim, H. I. Lee, Appl. Catal. A:General, **281**, 167 (2005).
[16] Q. Y. Liu, W. L. Wu, J. Wang, X. Q. Ren, Y. R. Wang, Microporous Mesoporous Mater. **76**, 51 (2004).
[17] P. M. Rao, A. Wolfson, S. Kababya, S. Vega, M. V. Landau, J. Catal. **232**, 210 (2005).
[18] P. M. Rao, M. V. Landau, A. Wolfson, A. M. Shapira-Tchelet, M. Herskowitz, Microporous Mesoporous Mater. **80**, 43 (2005).
[19] K. Nowinska, R. Formaniak, W. Kaleta, A. Waclaw, Appl. Catal. A:General **256,** 115 (2003).
[20] A. Lapkin, B. Bozkaya, T. Mays, L. Borello, K. Edler, B. Crittenden, Catal. Today **81**, 611 (2003).
[21] S. C. Laha, P. Mukherjee, S. R. Sainkar, R. Kumar, J. Catal. **207**, 213 (2002).

*Corresponding author: alpopa_tim2003@yahoo.com